energies

MDPI

Article

Integrated Optimal Dispatch of a Rural Micro-Energy-Grid with Multi-Energy Stream Based on Model Predictive Control

Xin Zhang [1,2], Jianhua Yang [1,*], Weizhou Wang [3], Man Zhang [1] and Tianjun Jing [1]

[1] College of Information and Electrical Engineering, China Agricultural University, Beijing 100083, China; zhangxin19861986@126.com (X.Z.); cauzm@cau.edu.cn (M.Z.); jtjy11@cau.edu.cn (T.J.)
[2] School of Information Engineering, Inner Mongolia University of Science & Technology, Baotou 014010, China
[3] State Grid Gansu Electric Power Company, Lanzhou 730050, China; tiankongxia126@126.com
* Correspondence: yang.haag@163.com; Tel.: +86-106-273-6746

Received: 13 November 2018; Accepted: 5 December 2018; Published: 8 December 2018

Abstract: Due to the randomness of the intermittent distributed energy output and load demand of a micro-energy-grid, micro-sources cannot fully follow the day-ahead micro-energy-grid optimal dispatching plan. Therefore, a micro-energy-grid is difficult to operate steadily and is challenging to include in the response dispatch of a distribution network. In view of the above problems, this paper proposes an integrated optimal dispatch method for a micro-energy-grid based on model predictive control. In the day-ahead optimal dispatch, an optimal dispatch model of a micro-energy-grid is built taking the daily minimum operating cost as the objective function, and the optimal output curve of each micro-source of the next day per hour is obtained. In the real-time dispatch, rolling optimization of the day-ahead optimal dispatching plan is implemented based on model predictive control theory. The real-time state of the system is sampled, and feedback correction of the system is implemented. The influence of uncertain factors in the system is eliminated to ensure steady operation of the system. Finally, the validity and feasibility of the integrated optimal dispatching method are verified by a case simulation analysis.

Keywords: multi-energy stream; micro-energy-grid; model predictive control; optimal dispatch; real-time dispatch

1. Introduction

With the gradual depletion of energy and increasingly salient environmental problems, the proportion of renewable energy consumption is increasing. All the countries in the world give an increased importance to renewable energy technology research. Renewable energy technology has become a hot topic in the energy field [1–4]. American futurist Jeremy Rifkin proposes the concept of the energy Internet [5]. Scholars promote the transformation of smart grids to the energy Internet [6–9], focusing not only on the clean utilization of electricity but also on the integrated utilization of cooling—heating-electricity-gas energy [10–15]. Then, the concept of micro-energy-grid is proposed. The micro-energy-grid is the natural extension of the microgrid. As a subsystem of the energy Internet, the micro-energy-grid is composed mainly of an electric power grid, a cooling and heating energy grid, a gas grid and other energy streams. The micro-energy-grid is applied in urban communities, industrial parks, rural areas and other areas. The micro-energy-grid uses electricity-heating-cooling storage and achieves conversion of cooling-heating-electricity-gas multi-energy, which is the main way to consume renewable energy [16,17]. Rural areas in China are rich in biomass energy, which has caused serious environmental pollution. At the same time, the utilization efficiency of biomass

energy is low. Renewable energy is abundant in rural areas of China, but the existing rural power grid is weak, and photovoltaic (PV) and wind power poverty alleviation facilities are insufficient. Therefore, the study of the rural micro-energy-grid optimal dispatch can achieve local rational utilization of biomass energy and renewable energy and improve the rural environment. Therefore, the micro-energy-grid is of great significance to the construction and development of new countryside.

Researchers working on the optimal dispatch of the microgrid have conducted substantial research [18–24]. For example, in [18], a bilevel optimal algorithm for microgrid clusters based on the alternating direction method of multipliers is proposed to achieve coordinated optimization for a multi-microgrid. In [19], a multi-objective optimal dispatching method for an isolated microgrid considering flexibility is proposed to improve the ability of the system to address the uncertainty of PV and wind power. In [20,21], the optimal operation methods for a microgrid are proposed based on the improved adaptive evolutionary algorithm and swarm optimization algorithm. In [22], considering the uncertain factors of renewable energy generation and price, a dispatching method of a reconfigurable microgrid based on uncertainty risk is proposed to achieve the benefit maximization of microgrid operators. In [23], an alternating direction method of multipliers based distributed algorithm is proposed to solve the economic dispatch model of the islanded microgrids. In [24], considering the random charging influence of electric vehicles on the microgrid, a multi-objective optimal dispatching model based on improved particle swarm optimization is proposed. Three different dispatching scenarios are established, and the corresponding dispatching results are discussed. Finally, the validity of the model is verified by case study. However, the above references focus on electric energy. The typical scenario of a cooling-heating-electricity-gas multi-energy stream micro-energy-grid is not considered. In [25], the day-ahead optimal dispatching model of the micro-energy-grid based on an energy hub is built to achieve optimal operation of the cooling-heating-electricity-gas multi-energy stream. In [26], a non-cooperative game model of micro-energy-grid and user is established based on game theory, and a method for solving the game model is proposed to achieve the economic operation of the micro-energy-grid. In [27], a two-stage stochastic mixed-integer linear programming model is proposed for the optimal dispatch of the micro-energy-grid. In [28], considering the demand-side response, a bilevel optimal scheduling model of the micro energy network based on the load aggregator business is proposed and verified by simulation. In [29,30], the optimal dispatching model of a PV agricultural greenhouse micro-energy-grid is proposed to simultaneously maximize the PV energy consumption and heat the greenhouse. Although the abovementioned references have achieved the day-ahead optimal dispatch of the cooling-heating-electricity-gas micro-energy-grid, the micro-sources cannot fully follow the day-ahead optimal dispatching plan of the micro-energy-grid due to the randomness of the intermittent distributed energy output and load demand. Thus, the operating results may not match the actual operation of the system. The micro-energy-grid is difficult to operate smoothly, and participation of the grid in the response dispatch of the distribution network is challenging.

In general, the recent studies have the following problems. (1) The research objective relates to the single-energy network represented by electrical energy. The demand of coordinated utilization of cooling-heating-electricity-gas multi-energy stream is difficult to satisfy. (2) Some of the above references study cooling-heating-electricity-gas multi-energy stream and achieve the day-ahead optimal dispatch of the cooling-heating-electricity-gas micro-energy-grid. However, due to the randomness of the intermittent distributed energy output and load demand, the micro-sources cannot fully follow the day-ahead optimal dispatching plan of the micro-energy-grid. Thus, the operating results may not match the actual operation of the system. The micro-energy-grid is difficult to operate smoothly, and participation in the response dispatch of the distribution network is challenging. (3) The research on rural micro-energy-grids is beneficial for achieving local rational utilization of biomass energy and renewable energy. However, few studies of micro-energy-grids in rural areas of China have been reported.

In response to the above problems, this paper makes the following contributions:

(1) The energy-supply architecture of the micro-energy-grid, including wind, PV, micro-turbine, and other micro-sources, is built, and the demand of cooling-heating-electricity load is considered.

(2) An integrated optimal dispatching method based on model predictive control for the micro-energy-grid, which divides the optimal dispatching process into the day-ahead optimal dispatch and the real-time optimal dispatch, is proposed. In the day-ahead optimal dispatch, the optimal dispatch model of the micro-energy-grid is built taking the daily minimum operating cost as the objective function, and the hourly optimal output curve of each micro-source in the next day is obtained. In the real-time optimal dispatch, based on the model predictive control theory, taking the day-ahead optimal dispatching results as the reference values, intraday multi-period rolling optimization and sampling real-time system state for feedback correction are conducted.

(3) In this study, the energy-supply architecture of the proposed energy grid is suitable for the rural areas of China. Biogas, PV energy and other biomass and renewable energy sources are used to achieve the integrated utilization of all kinds of resources in rural areas.

The remainder of this paper is structured as follows: Section 2 establishes the energy-supply architecture of the micro-energy-grid and presents the components and operating mechanism of the micro-energy-grid. In Section 3, an integrated dispatching framework of the micro-energy-grid is built based on model predictive control, and the integrated dispatching method of the micro-energy-grid is outlined. In Section 4, an integrated optimal dispatching model of the micro-energy-grid, including the day-ahead and real-time optimal dispatching model, is built. In Section 5, a case study is used to validate the proposed model. The full paper is summarized and future work is predicted in Section 6. The general workflow of the integrated optimal dispatch of the rural micro-energy-grid with multi-energy stream based on model predictive control is shown in Figure 1.

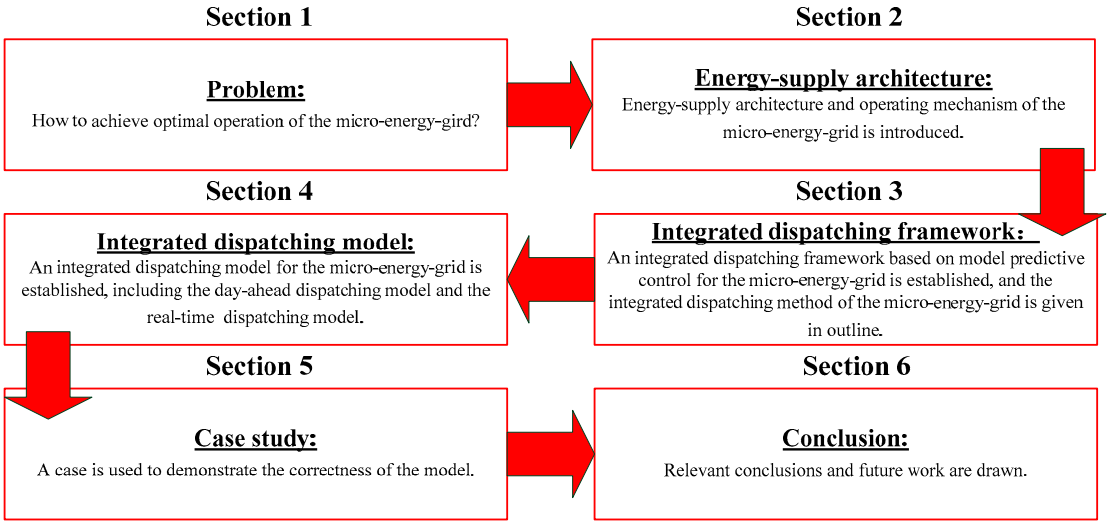

Figure 1. General workflow for the integrated optimal dispatch of the rural micro-energy-grid with multi-energy stream based on model predictive control.

2. Components and Energy-Supply Mechanism of Rural Micro-Energy-Grid

In this paper, the cooling-heating-electricity-gas multi-energy stream micro-energy-grid includes wind and PV power generation system, micro-turbine, biogas-fired boiler, heat-recovery boiler, lithium-bromide absorption-type refrigerators, battery storage device, cooling and heating storage device, and air-source heat pump. The energy-supply architecture of the system is shown in Figure 2.

The micro-energy-grid is connected to the external distribution network. When the electricity energy supply of the micro-turbine, wind and PV power generation system is larger than the internal electrical load, electrical energy is sold to the external distribution network, and the battery is charged.

When the electricity energy supply of the abovementioned device is less than the internal electrical load, electrical energy is purchased from the external distribution network, and the battery storage is discharged. The function of the battery storage device is peak load shifting. The heating load is satisfied by the heat-recovery boiler, biogas-fired boiler and air-source heat pump. The raw material of the heating device is provided by the biogas generated by biomass waste and rural natural air. When the heating energy supply of the micro-energy-grid exceeds the internal heating load, the heating storage device is charged. When the heating energy supply of the micro-energy-grid is less than the internal heating load, the heating storage device is discharged. The function of the heating storage is peak load shifting. The cooling load is satisfied by the lithium-bromide absorption-type refrigerator and air-source heat pump. When the cooling energy supply of the micro-energy-grid exceeds the internal cooling load, the cooling storage device is charged. When the cooling energy supply of the micro-energy-grid is less than the internal cooling load, the cooling storage device is discharged. The function of the cooling storage is peak load shifting.

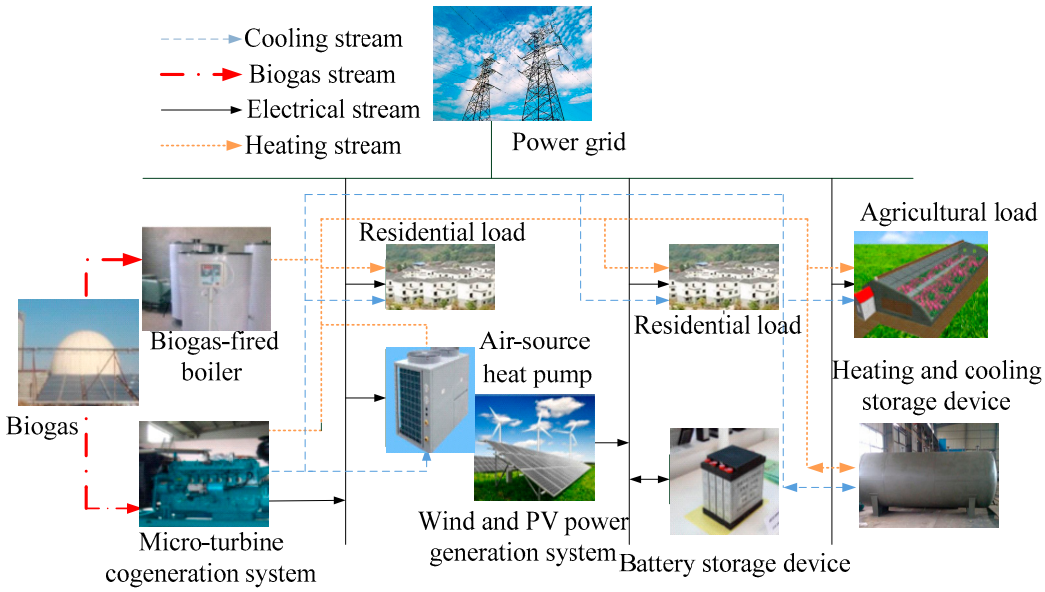

Figure 2. Energy-supply architecture of the micro-energy-grid.

3. Integrated Optimal Dispatching Framework of the Micro-Energy-Grid Based on Model Predictive Control

The accurate curves of the intermittent renewable energy output and load demand are built by the accurate prediction. However, as the predictive time scale increases, the predictive accuracy of the wind and PV power generation system decreases, as well as the load, resulting in a large deviation between the day-ahead optimal dispatching strategy and actual operation, which cannot satisfy the actual dispatching requirement of the system. Thus, an integrated optimal dispatching method for the micro-energy-grid based on model predictive control is proposed in this paper. The integrated optimal dispatch includes the day-ahead optimal dispatch and real-time optimal dispatch. The integrated optimal dispatching framework of the micro-energy-grid is shown in Figure 3.

(1) Day-ahead optimal dispatch

Based on the day-ahead predictive curve of the wind and PV power generation system as well as load, and considering the characteristics of each micro-source and the relevant constraints, the daily minimum operating cost of the micro-energy-grid is taken as the objective function. The hourly optimal output curve of each micro-source in the next day is obtained. The charge and discharge curves of the energy storage device and the hourly power exchange curve of the micro-energy-grid and the distribution network in the next day are also obtained.

(2) Real-time optimal dispatch

Rolling optimization of the intraday real-time optimal dispatching plan is performed by taking 5 min as a period to eliminate the actual intraday operating deviation caused by the large predictive error, and the ultra-short-term predictive information of the wind and PV power generation system as well as load is considered simultaneously. Based on model predictive control theory, the correction plans of all the micro-sources in the time window (the time window includes many periods) are obtained. In each time segment, the corrected dispatching plan of the next period is issued. In the next 5-min period, the above-mentioned process will be repeated, and the operating state of the system is sampled in real time to implement the feedback correction of the system.

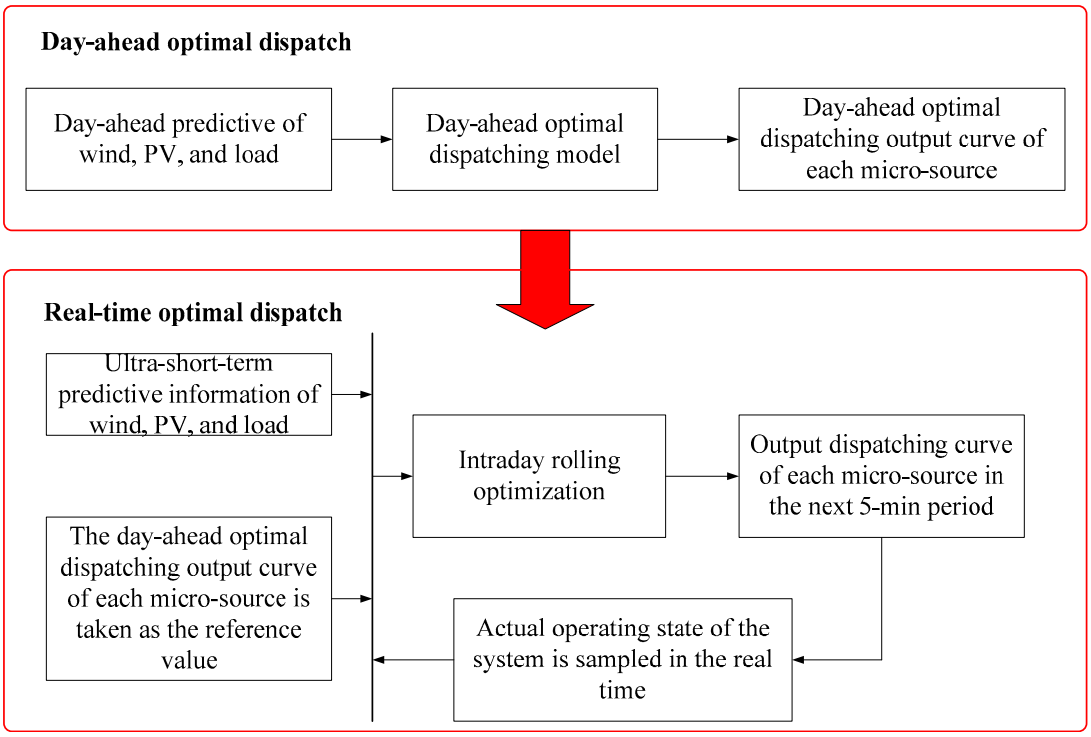

Figure 3. Integrated optimal dispatching framework of the rural micro-energy-grid.

4. Integrated Optimal Dispatching Model of the Rural Micro-Energy-Grid

4.1. Day-Ahead Optimal Dispatching Model

In this study, the biogas is provided by the rural biogas supply station. The sources of the raw materials are rural straw, animal waste and other kinds of biomass waste. Therefore, the daily operating cost of the proposed rural micro-energy-grid includes mainly the cost of purchasing electricity from the distribution network and selling electricity to the distribution network, the converting cost of environment pollution, the maintenance cost of the system, and the cost of purchasing biogas. The daily minimum operating cost of the micro-energy-grid is taken as the objective function in the day-ahead optimal dispatch. The objective function is as follows:

$$\min C = \min(C_{\text{elertri}} + C_{\text{maintain}} + C_{\text{pollution}} + C_{\text{gas}} + C_{\text{estor}}) \quad (1)$$

$$C_{\text{elertri}} = \sum_{t=1}^{24} \left(\frac{e_1(t) + e_2(t)}{2} P_{ex}(t) + \frac{e_1(t) - e_2(t)}{2} |P_{\text{ex}}(t)| - e_3(t)(P_{\text{PV}}(t) + P_{\text{WT}}(t)) - e_4(t) P_{\text{MT}}(t)\right) \quad (2)$$

$$C_{\text{maintain}} = \sum_{t=1}^{24} C_{mEB} P_{\text{EB}}(t) + \sum_{t=1}^{24} C_{mGB} P_{\text{GB}}(t) + \sum_{t=1}^{24} C_{mWT} P_{\text{WT}}(t) + \sum_{t=1}^{24} C_{mAC} P_{\text{AC}}(t) + \sum_{t=1}^{24} C_{mASHP} P_{\text{CASHP}}(t) + \sum_{t=1}^{24} C_{mcstor} |P_{\text{cstor}}(t)| + \sum_{t=1}^{24} C_{mMT} P_{\text{MT}}(t) + \sum_{t=1}^{24} C_{mPV} P_{\text{PV}}(t) + \sum_{t=1}^{24} C_{mASHP} P_{\text{HASHP}}(t) + \sum_{t=1}^{24} C_{mhstor} |P_{\text{hstor}}(t)| \tag{3}$$

$$C_{\text{pollution}} = \sum_{y=1}^{m} (C_y + D_y) B_y (P_{MT}(t) + P_{GB}(t)) \tag{4}$$

$$C_{\text{gas}} = C_{\text{fuel}} (P_{\text{MT}}(t) + P_{\text{GB}}(t)) \tag{5}$$

$$C_{\text{estor}} = \sum_{t=1}^{24} (C_{mestor1} + C_{mestor2}) |P_{\text{estor}}(t)| \tag{6}$$

The constraint conditions that must be satisfied by the day-ahead optimal dispatch are as follows:

(1) Electrical power balance constraint condition:

$$P_{\text{estor}}(t) + P_{\text{MT}}(t) + P_{\text{ex}}(t) = P_{\text{electriload}}(t) + P_{\text{ASHP}}(t) - P_{\text{WT}}(t) - P_{\text{PV}}(t) \tag{7}$$

(2) Heating power balance constraint condition:

$$P_{\text{HASHP}}(t) + P_{\text{EB}}(t) + P_{\text{GB}}(t) + P_{\text{hstor}}(t) = P_{\text{heatingload}}(t) \tag{8}$$

(3) Cooling power balance constraint condition:

$$P_{\text{CASHP}}(t) + P_{\text{AC}}(t) + P_{\text{cstor}}(t) = P_{\text{coolingload}}(t) \tag{9}$$

(4) Micro-turbine constraint conditions:

$$0 \le P_{\text{MT}}(t) \le P_{\text{MT}}^{\max} \tag{10}$$

$$-R_{\text{MT}}^{\text{down}} \le P_{\text{MT}}(t) - P_{\text{MT}}(t-1) \le R_{\text{MT}}^{\text{up}} \tag{11}$$

(5) Heat-recovery boiler constraint conditions:

$$P_{\text{EB}}(t) = \frac{P_{\text{MT}}(t)(1 - \eta_{\text{e}} - \eta_1)\eta_{\text{rec}}\eta_{\text{EB}}}{\eta_{\text{e}}} \tag{12}$$

$$0 \le P_{\text{EB}}(t) \le P_{\text{EB}}^{\max} \tag{13}$$

(6) Biogas-fired boiler constraint conditions:

$$0 \le P_{\text{GB}}(t) \le P_{\text{GB}}^{\max} \tag{14}$$

$$-R_{\text{GB}}^{\text{down}} \le P_{\text{GB}}(t) - P_{\text{GB}}(t-1) \le R_{\text{GB}}^{\text{up}} \tag{15}$$

(7) Lithium-bromide absorption-type refrigerator constraint conditions:

$$P_{\text{AC}}(t) = \frac{P_{\text{MT}}(t)(1 - \eta_{\text{e}} - \eta_1)\eta_{\text{rec}}\eta_{\text{AC}}\eta_{\text{EB}}}{\eta_{\text{e}}} \tag{16}$$

$$0 \le P_{\text{AC}}(t) \le P_{\text{AC}}^{\max} \tag{17}$$

(8) Cooling-heating-electricity storage device constraint conditions: Because the functions and principles of the battery storage device and the cooling and heating storage device are similar, their general models are as follows:

$$S_{\text{stor}}(t) = S_{\text{stor}}(t-1)(1-\delta) + \Delta T P_{\text{ch}}(t)\eta_{\text{ch}}/E_{\text{tstor}} - \Delta T P_{\text{dis}}(t)/(\eta_{\text{dis}}E_{\text{tstor}}) \tag{18}$$

$$S_{\text{stor}}^{\min} \le S_{\text{stor}}(t) \le S_{\text{stor}}^{\max} \tag{19}$$

$$S_{\text{stor}}(0) = S_{\text{stor}}(T) \tag{20}$$

$$0 \le P_{\text{dis}}(t) \le P_{\text{dmax}} \tag{21}$$

$$0 \le P_{\text{ch}}(t) \le P_{\text{cmax}} \tag{22}$$

$$P_{\text{stor}}(t) = \begin{cases} P_{\text{ch}}(t), P_{\text{stor}}(t) \ge 0 \\ -P_{\text{dis}}(t), P_{\text{stor}}(t) < 0 \end{cases} \tag{23}$$

(9) Air-source heat pump constraint conditions:

$$P_{\text{HASHP}}(t) = D_{\text{HASHP}}P_{\text{ASHP}}(t) \tag{24}$$

$$P_{\text{CASHP}}(t) = D_{\text{CASHP}}P_{\text{ASHP}}(t) \tag{25}$$

$$0 \le P_{\text{ASHP}}(t) \le P_{\text{ASHP}}^{\max} \tag{26}$$

(10) Power exchange between the micro-energy-grid and the distribution network constraint condition:

$$P_{\text{ex}}^{\min} \le P_{\text{ex}}(t) \le P_{\text{ex}}^{\max} \tag{27}$$

(11) Reserve power constraint condition:

$$P_{\text{WT}}^{\max} + P_{\text{PV}}^{\max} + P_{\text{MT}}^{\max} + P_{\text{ex}}^{\max} \ge P_{\text{electriload}}(t)(1+\Upsilon_{\text{res}}) \tag{28}$$

4.2. Real-Time Optimal Dispatching Model

Model predictive control is a closed-loop optimal control method that includes model prediction, rolling optimization and feedback correction. This strategy includes the following steps. (1) At current time k and current state $x(k)$, the future state of the system is predicted based on the predictive model. Based on the above analytical results, considering the current and future constraints, the control order sequence of the future time $k+\Delta t, k+2\Delta t, ..., k+N\Delta t$ is obtained by solving the optimization control objective function. (2) The first value of the control instruction sequence is applied to the control system. (3) At time $k+\Delta t$, the state is updated to $x(k+\Delta t)$, and the above steps are repeated. In this paper, an intraday real-time optimal dispatching model is built to achieve the optimal coordinated intraday dispatch of each micro-source based on model predictive control theory.

4.2.1. Predictive Model

The control variables are obtained by solving the rolling optimization model. The output curves of the micro-source and storage are predicted in the future time-limited region. The specific predictive model is as follows:

$$\begin{cases} P_{\mathrm{EB}}(k+n\Delta t) = P_{\mathrm{EB}}(k) + \sum\limits_{t=\Delta t}^{n\Delta t} \Delta P_{EB}(k+t) \\ P_{\mathrm{GB}}(k+n\Delta t) = P_{\mathrm{GB}}(k) + \sum\limits_{t=\Delta t}^{n\Delta t} \Delta P_{GB}(k+t) \\ P_{\mathrm{AC}}(k+n\Delta t) = P_{\mathrm{AC}}(k) + \sum\limits_{t=\Delta t}^{n\Delta t} \Delta P_{AC}(k+t) \\ P_{\mathrm{MT}}(k+n\Delta t) = P_{\mathrm{MT}}(k) + \sum\limits_{t=\Delta t}^{n\Delta t} \Delta P_{MT}(k+t) \\ P_{\mathrm{ASHP}}(k+n\Delta t) = P_{\mathrm{ASHP}}(k) + \sum\limits_{t=\Delta t}^{n\Delta t} \Delta P_{ASHP}(k+t) \\ P_{\mathrm{estor}}(k+n\Delta t) = P_{\mathrm{estor}}(k) + \sum\limits_{t=\Delta t}^{n\Delta t} \Delta P_{estor}(k+t) \\ P_{\mathrm{cstor}}(k+n\Delta t) = P_{\mathrm{cstor}}(k) + \sum\limits_{t=\Delta t}^{n\Delta t} \Delta P_{cstor}(k+t) \\ P_{\mathrm{hstor}}(k+n\Delta t) = P_{\mathrm{hstor}}(k) + \sum\limits_{t=\Delta t}^{n\Delta t} \Delta P_{hstor}(k+t) \\ S_{\mathrm{estor}}(k+n\Delta t) = (1-\sigma_{\mathrm{estor}}) S_{\mathrm{estor}}(k+(n-1)\Delta t) - \frac{\Delta T \eta_{\mathrm{estor}}}{E_{\mathrm{testor}}} P_{\mathrm{estor}}(k+n\Delta t) \\ S_{\mathrm{cstor}}(k+n\Delta t) = (1-\sigma_{\mathrm{cstor}}) S_{\mathrm{cstor}}(k+(n-1)\Delta t) - \frac{\Delta T \eta_{\mathrm{cstor}}}{E_{\mathrm{tcstor}}} P_{\mathrm{cstor}}(k+n\Delta t) \\ S_{\mathrm{hstor}}(k+n\Delta t) = (1-\sigma_{\mathrm{hstor}}) S_{\mathrm{hstor}}(k+(n-1)\Delta t) - \frac{\Delta T \eta_{\mathrm{hstor}}}{E_{\mathrm{thstor}}} P_{\mathrm{hstor}}(k+n\Delta t) \\ P_{\mathrm{ex}}(k+n\Delta t) = P_{\mathrm{ex}}(k) - \sum\limits_{t=\Delta t}^{n\Delta t} \Delta P_{MT}(k+t) - \sum\limits_{t=\Delta t}^{n\Delta t} \Delta P_{estor}(k+t) - \sum\limits_{t=\Delta t}^{n\Delta t} \Delta P_{WT}(k+t) - \sum\limits_{t=\Delta t}^{n\Delta t} \Delta P_{PV}(k+t) + \sum\limits_{t=\Delta t}^{n\Delta t} \Delta P_{electriload}(k+t) + \sum\limits_{t=\Delta t}^{n\Delta t} \Delta P_{ASHP}(k+t) \\ n = 1,2,\cdots,N \end{cases} \tag{29}$$

4.2.2. Objective Function (Rolling Optimization)

In this paper, the minimum variations in the intraday power exchange between the micro-energy-grid and the distribution network, the state of charge of the cooling-heating-electricity storage device, and the energy-supply units are taken as the objective function. The real-time optimal dispatching model is built based on model predictive control. The objective function is as follows:

$$\begin{aligned} \min J = & \sum_{t=\Delta t}^{N\Delta t} (P_{ex}(k+t) - \hat{P}_{ex}(k+t))^2 + \sum_{t=\Delta t}^{N\Delta t} (S_{estor}(k+t) - \hat{S}_{estor}(k+t))^2 + \sum_{t=\Delta t}^{N\Delta t} (S_{cstor}(k+t) - \hat{S}_{cstor}(k+t))^2 + \\ & \sum_{t=\Delta t}^{N\Delta t} (S_{hstor}(k+t) - \hat{S}_{hstor}(k+t))^2 + \sum_{t=\Delta t}^{N\Delta t} (P_{estor}(k+t) - \hat{P}_{estor}(k+t))^2 + \sum_{t=\Delta t}^{N\Delta t} (P_{cstor}(k+t) - \hat{P}_{cstor}(k+t))^2 + \\ & \sum_{t=\Delta t}^{N\Delta t} (P_{hstor}(k+t) - \hat{P}_{hstor}(k+t))^2 + \sum_{t=\Delta t}^{N\Delta t} (P_{EB}(k+t) - \hat{P}_{EB}(k+t))^2 + \sum_{t=\Delta t}^{N\Delta t} (P_{GB}(k+t) - \hat{P}_{GB}(k+t))^2 + \\ & \sum_{t=\Delta t}^{N\Delta t} (P_{AC}(k+t) - \hat{P}_{AC}(k+t))^2 + \sum_{t=\Delta t}^{N\Delta t} (P_{MT}(k+t) - \hat{P}_{MT}(k+t))^2 + \sum_{t=\Delta t}^{N\Delta t} (P_{ASHP}(k+t) - \hat{P}_{ASHP}(k+t))^2 \end{aligned} \tag{30}$$

When rolling optimization is performed, the system state is sampled in real time, which is equivalent to a certain amount of feedback correction effect. The constraint conditions that must be satisfied by the real-time optimal dispatch are as follows:

(1) The controllable unit constraint conditions:

$$\begin{cases} \Delta P_{\mathrm{EB}}^{\min} \le \Delta P_{\mathrm{EB}}(k+t) \le \Delta P_{\mathrm{EB}}^{\max} \\ \Delta P_{\mathrm{GB}}^{\min} \le \Delta P_{\mathrm{GB}}(k+t) \le \Delta P_{\mathrm{GB}}^{\max} \\ \Delta P_{\mathrm{AC}}^{\min} \le \Delta P_{\mathrm{AC}}(k+t) \le \Delta P_{\mathrm{AC}}^{\max} \\ \Delta P_{\mathrm{MT}}^{\min} \le \Delta P_{\mathrm{MT}}(k+t) \le \Delta P_{\mathrm{MT}}^{\max} \\ \Delta P_{\mathrm{ASHP}}^{\min} \le \Delta P_{\mathrm{ASHP}}(k+t) \le \Delta P_{\mathrm{ASHP}}^{\max} \\ 0 \le P_{\mathrm{EB}}(k+n\Delta t) \le P_{\mathrm{EB}}^{\max} \\ 0 \le P_{\mathrm{GB}}(k+n\Delta t) \le P_{\mathrm{GB}}^{\max} \\ 0 \le P_{\mathrm{AC}}(k+n\Delta t) \le P_{\mathrm{AC}}^{\max} \\ 0 \le P_{\mathrm{MT}}(k+n\Delta t) \le P_{\mathrm{MT}}^{\max} \\ 0 \le P_{\mathrm{ASHP}}(k+n\Delta t) \le P_{\mathrm{ASHP}}^{\max} \\ n = 1,2,\cdots,N \end{cases} \tag{31}$$

(2) The electricity–cooling–heating storage device constraint conditions:

$$\begin{cases} \Delta P_{\text{estor}}^{\min} \le \Delta P_{\text{estor}}(k+t) \le \Delta P_{\text{estor}}^{\max} \\ \Delta P_{\text{cstor}}^{\min} \le \Delta P_{\text{cstor}}(k+t) \le \Delta P_{\text{cstor}}^{\max} \\ \Delta P_{\text{hstor}}^{\min} \le \Delta P_{\text{hstor}}(k+t) \le \Delta P_{\text{hstor}}^{\max} \\ P_{\text{estor}}^{\min} \le P_{\text{estor}}(k+n\Delta t) \le P_{\text{estor}}^{\max} \\ P_{\text{cstor}}^{\min} \le P_{\text{cstor}}(k+n\Delta t) \le P_{\text{cstor}}^{\max} \\ P_{\text{hstor}}^{\min} \le P_{\text{hstor}}(k+n\Delta t) \le P_{\text{hstor}}^{\max} \\ S_{\text{estor}}^{\min} \le S_{\text{estor}}(k+n\Delta t) \le S_{\text{estor}}^{\max} \\ S_{\text{cstor}}^{\min} \le S_{\text{cstor}}(k+n\Delta t) \le S_{\text{cstor}}^{\max} \\ S_{\text{hstor}}^{\min} \le S_{\text{hstor}}(k+n\Delta t) \le S_{\text{hstor}}^{\max} \\ n = 1, 2, \cdots, N \end{cases} \tag{32}$$

4.3. Integrated Optimal Dispatching Model Solution

The solution steps of the integrated optimal dispatch of rural micro-energy-grid based on model predictive control are shown in Figure 4.

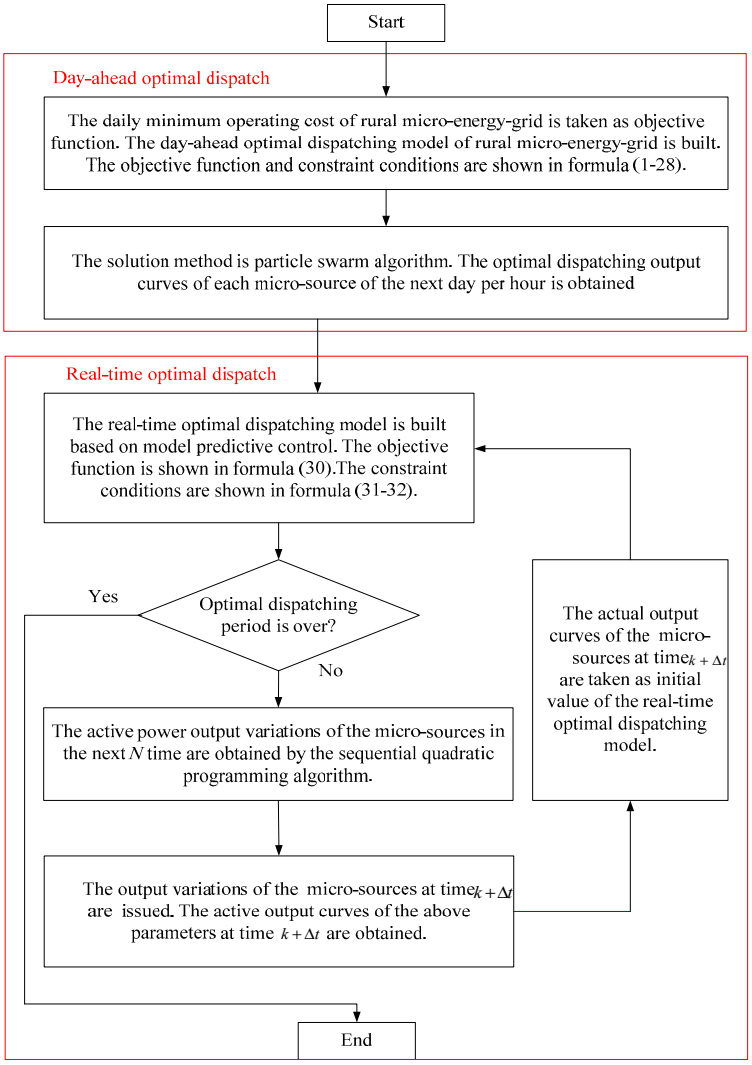

Figure 4. Integrated optimal dispatching solution workflow of the rural micro-energy-grid.

(1) The daily minimum operating cost of the rural micro-energy-grid is taken as the objective function, and the day-ahead optimal dispatching model of the rural micro-energy-grid is built. The problem is solved using the particle swarm algorithm, and the hourly optimal dispatching output curves in the next day are obtained for each micro-source.

(2) The power output curves of the micro-sources in the day-ahead optimal dispatch are taken as the reference values. The real-time optimal dispatching model is built based on model predictive control. The active power output variations of the micro-sources in the next N time are obtained by the sequential quadratic programming algorithm.

(3) The power output variations of the micro-sources at time $k + \Delta t$ are issued, and the active power output curves of the micro-sources at time $k + \Delta t$ are obtained.

(4) The actual power output curves of the micro-sources at time $k + \Delta t$ are taken as the initial values of the real-time optimal dispatching model. The process then returns to Step 2, and a new round of optimization is performed.

5. Case Study

A village in western China was taken as a case. According to the actual situation of the region, electrical and heating energy are supplied in winter, and electrical and cooling energy are supplied in summer. The electricity price of the power grid is based on the time-of-use electrical price issued by Gansu Province Development and Reform Commission in China. Electricity is sold to the distribution network at a price of 0.65 (RMB·(kW·h)$^{-1}$). The purchasing price of biogas is 0.35 (RMB·(kW·h)$^{-1}$). The value of the power generation efficiency of the micro-turbine η_e is 0.26, the value of the heating loss coefficient of the micro-turbine η_1 is 0.03, and the value of the recovery efficiency of the flue gas waste heat η_{rec} is 0.55 [31]. The lithium battery storage device was adopted in this case study. The cost for storing energy in lithium battery is 0.2 (RMB·(kW·h)$^{-1}$). The parameters of the energy-supply device [32,33] are shown in Table 1. The maintenance costs [32,34,35] for the energy-supply device are shown in Table 2. The parameters of the electricity–cooling–heating storage device [32] are shown in Table 3. The electricity selling prices of the PV, wind and micro-turbine power generation system are shown in Table 4. The electricity selling price of the PV and wind power generation system contains government subsidy. The related parameters of environmental pollution are in [35]. The time-of-use electrical price of the power grid is shown in Figure 5. The predictive data of the wind and PV power generation system and the cooling-heating-electricity load were obtained by Monte Carlo simulation [36,37] of the day-ahead optimal dispatch. The predictive results of the day-ahead optimal dispatch are shown in Figure 6. To reflect the universality of the test parameters, the intraday ultra-short-term prediction data are the sum of the day-ahead predictive value and the predictive error, which has a normal distribution. The intraday ultra-short-term predictive results of the real-time optimal dispatch are shown in Figure 7. The parameters of the particle swarm algorithm were as follows: number of particles, 20; number of iterations, 50; learning factor, 2; period of the day-ahead optimal dispatch, 1 h; predictive and control times, 60 min; and period of rolling optimal dispatch, 5 min.

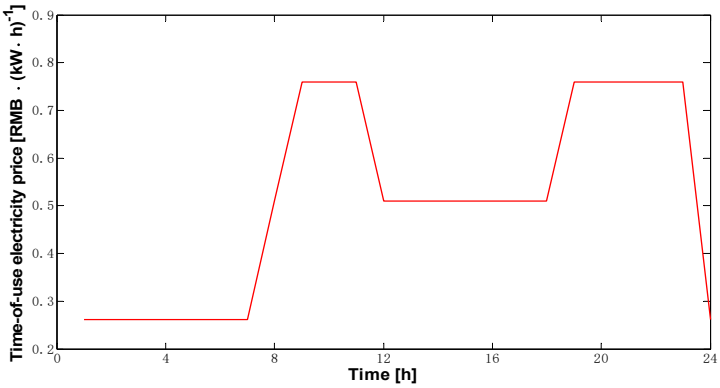

Figure 5. Time-of-use electrical price curve of the power grid.

Table 1. Parameters of the energy-supply device of the micro-energy-grid.

Device	Parameter	Value
Micro turbine(six)	Maximum generated power ($kW \cdot one^{-1}$)	100
	Rated efficiency	0.26
	Climbing speed ($kW \cdot min^{-1}$)	Upward 30, Downward 20
Heat-recovery boiler	Maximum input power (kW)	900
	Rated efficiency	0.9
Lithium-bromide absorption-type refrigerator	Maximum input power (kW)	900
	Rated efficiency	1.2
Biogas-fired boiler	Maximum input power (kW)	500
	Rated efficiency	0.8
	Climbing speed ($kW \cdot min^{-1}$)	Upward 30, Downward 20
Air-source heat pumps for heating and cooling exchange	Maximum heating and cooling exchange power (kW)	1000
	Heating and cooling efficiency parameter	3.7
Power exchange between micro-energy-grid with external power grid	Maximum exchange power (kW)	1000
PV power generation system	Maximum generated power (kW)	300
Wind power generation system	Maximum generated power (kW)	100

Table 2. Maintenance costs of the energy-supply device.

Device	Maintenance Cost ($RMB \cdot (kW \cdot h)^{-1}$)
Micro turbine	0.03
Heat-recovery boiler	0.02
Lithium-bromide absorption-type refrigerator	0.025
Biogas-fired boiler	0.02
Air-source heat pump	0.02
PV power generation system	0.03
Wind power generation system	0.03
Battery storage device	0.03
Heating storage device	0.02
Cooling storage device	0.02

Table 3. Parameters of electricity–cooling–heating storage device.

Storage Device Parameter	Electricity-Cooling-Heating Efficiency		Self-Discharging Efficiency of Cooling-Heating-Electricity	State of Charge of Cooling-Heating-Electricity		Capacity (kW·h)
	Max Charge	Max Discharge		Maximum	Minimum	
Battery storage device	0.2	0.2	0.02	0.9	0.2	1000
Heating storage device	0.2	0.2	0.03	0.9	0.1	1000
Cooling storage device	0.2	0.2	0.03	0.9	0.1	1000

Table 4. Electricity selling price of the PV, wind and micro-turbine power generation system.

Device	Price ($RMB \cdot (kW \cdot h)^{-1}$)
Micro turbine	0.2610 (23:00–24:00, 00:00–07:00) 0.5100 (07:00–08:00, 11:00–18:00) 0.7590 (08:00–11:00, 18:00–23:00)
PV and wind power generation system	0.8610 (23:00–24:00, 00:00–07:00) 1.1100 (07:00–08:00, 11:00–18:00) 1.3590 (08:00–11:00, 18:00–23:00)

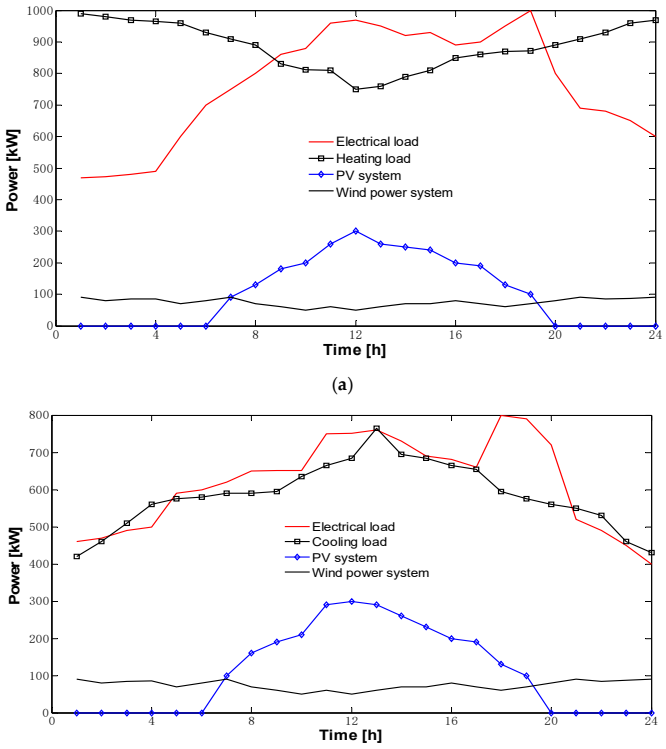

Figure 6. The day-ahead predictive data of the wind and PV power generation system, and the cooling-heating-electricity load in: winter (**a**); and summer (**b**).

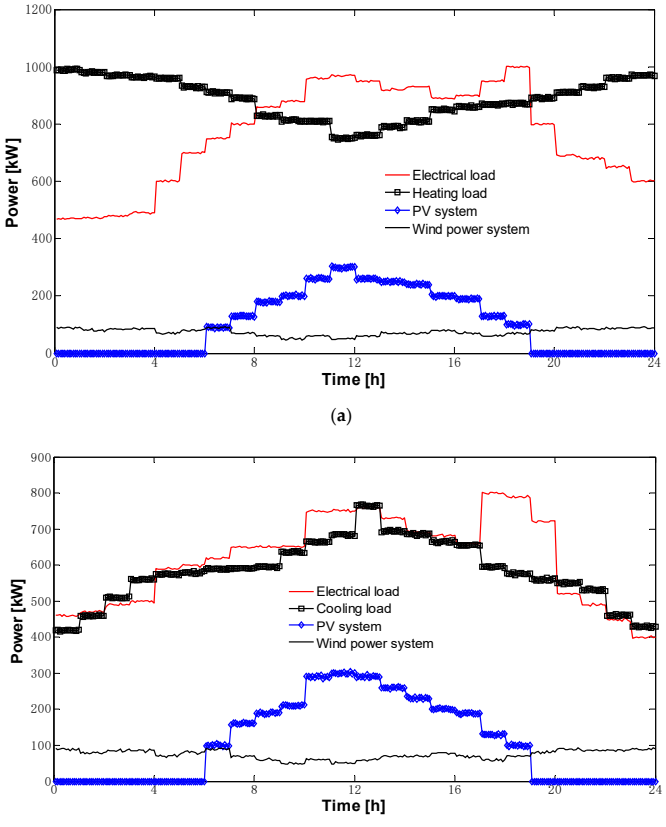

Figure 7. Intraday ultra-short-term predictive data of the wind and PV power generation system, and the cooling-heating-electricity load in: winter (**a**); and summer (**b**).

5.1. The Results of Day-Ahead Optimal Dispatch

The electrical load balance curves of a typical day in winter (Figure 8a) and summer (Figure 8b) under day-ahead optimal dispatching mode are shown in Figure 8. The output power curves of the micro-sources in winter and summer are similar. Therefore, Figure 8a is taken as an illustrative example. According to Figure 8a, during Periods 23–24 and 0–7, because the price of electricity is at the lowest point and is lower than the price of biogas, wind energy and the electricity purchased from the distribution network are used to satisfy the electrical load demand, and the battery storage device is fully charged. Battery storage is used to improve the economy of the system. In Periods 7–23, the price of electricity price is at the highest and exceeds the price of the biogas. The electricity purchasing cost of the micro-energy-grid is relatively high. Therefore, the micro-turbine, PV and wind power generation system become the main electricity-supply units. The battery storage device is discharged to satisfy the electrical load demand if the above units cannot satisfy the demand. The battery storage device is charged during periods of low electricity prices and low loads. The battery storage device is discharged in periods of high electricity prices and high loads. The function of the battery storage device, which is peak load shifting, is achieved, and the economy of the system is improved.

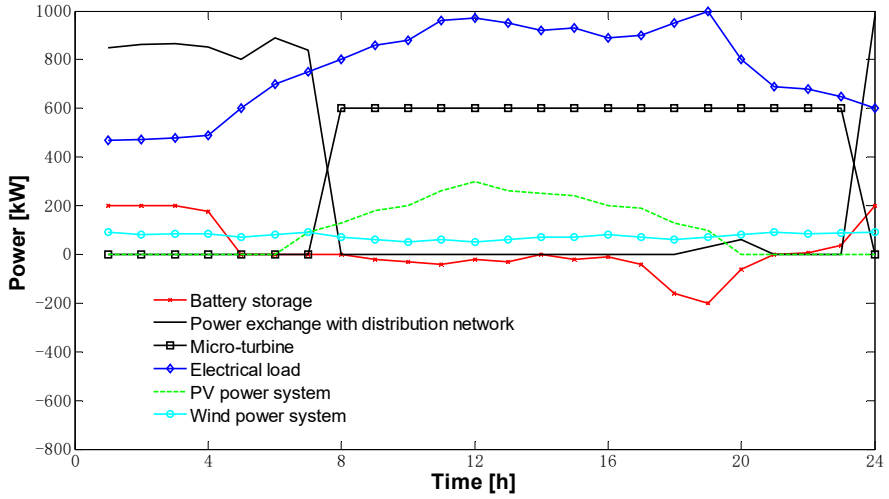

(**a**)

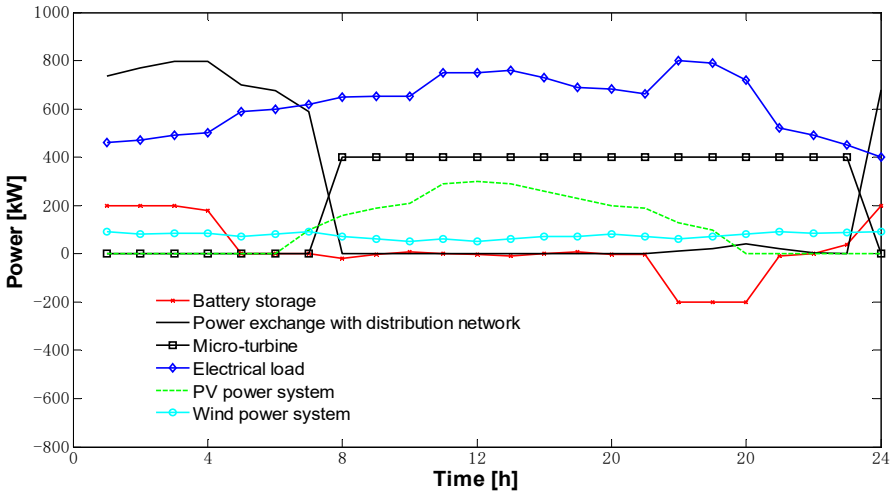

(**b**)

Figure 8. The electrical load balance curves of a typical day in winter (**a**) and summer (**b**) under day-ahead optimal dispatching mode.

The heating load balance curves of a typical day in winter (Figure 9a) and the cooling load balance curves of a typical day in summer (Figure 9b) under day-ahead optimal dispatching mode are shown in Figure 9. The output power curves of the micro-sources for the heating load in winter are similar to those of the micro-sources for the cooling load in summer. Therefore, Figure 9a is taken as an illustrative example. According to Figure 9a, during Periods 23–24 and 0–7, the price of electricity is at the lowest point of the day. The air-source heat pump and biogas-fired boiler are used to satisfy the heating load demand, and the heating storage device is fully charged. During Periods 7–23, the price of electricity is at the highest point of the day, and the heat-recovery boiler becomes the main heating-supply unit because insufficient electricity is supplied by the heating storage device and biogas-fired boiler. The heating storage device is charged during periods of low electricity prices and discharged during periods of high electricity prices to satisfy the demand of the system.

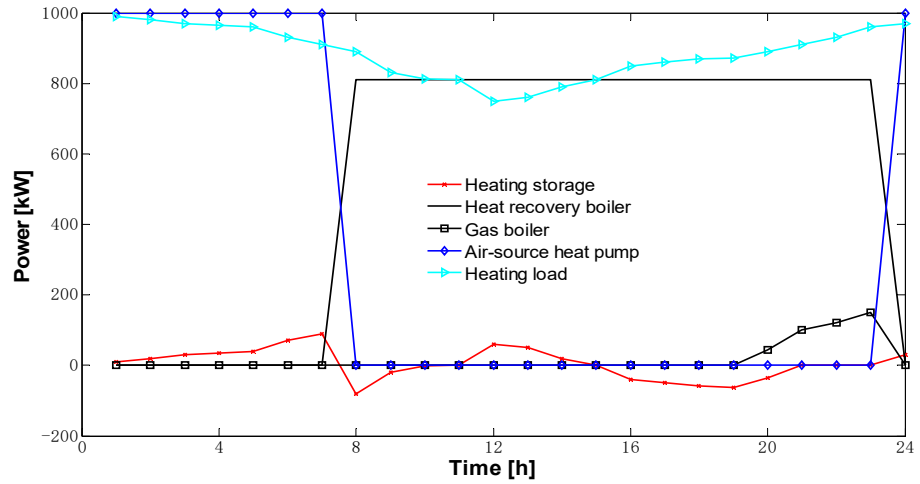

(**a**)

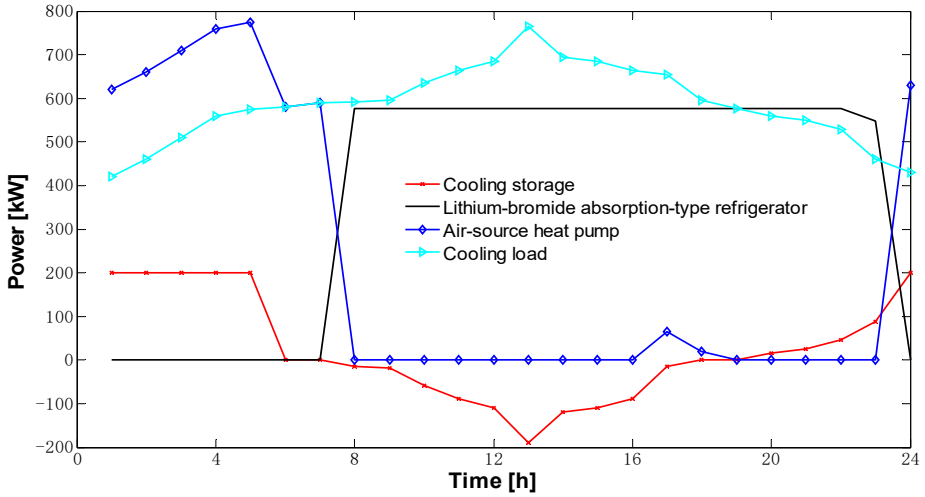

(**b**)

Figure 9. The heating load balance curves of a typical day in winter (**a**) and the cooling load balance curves of a typical day in summer (**b**) under day-ahead optimal dispatching mode.

5.2. The Results of Real-Time Optimal Dispatch

The electrical load balance curves of a typical day in winter (Figure 10a) and summer (Figure 10b) under real-time optimal dispatching mode are shown in Figure 10. According to Figure 8, the day-ahead optimal dispatch plan takes an hour as the time scale, but the dispatch is

extensive. The predictive error of renewable energy and electrical load and the influence of unplanned instantaneous power fluctuation on the control of the micro-energy-grid are not fully reflected. The system cannot respond to fluctuations in the renewable energy and load in time. According to Figure 10, the day-ahead optimal dispatch is improved upon by the real-time optimal dispatch. The real-time optimal dispatch is more accurate than the day-ahead optimal dispatch, and the output power of each electricity-supply unit has small fluctuation. The real-time optimal dispatch is more in line with the actual situation. Because the power of each electricity-supply unit has only a small change, safe operation of the system is guaranteed; meanwhile, the renewable energy and electrical load fluctuation are considered. Therefore, the micro-energy-grid can operate smoothly.

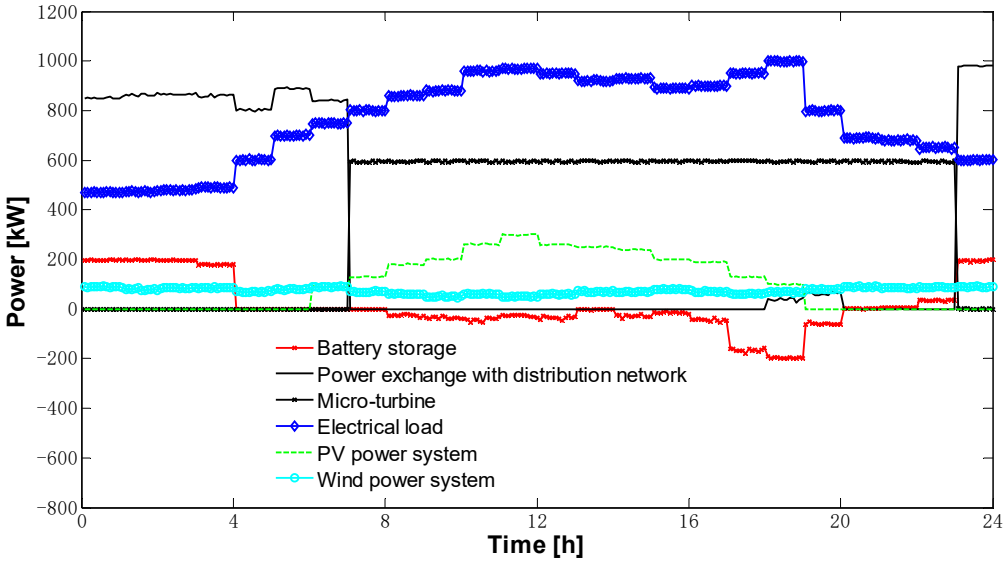

(**a**)

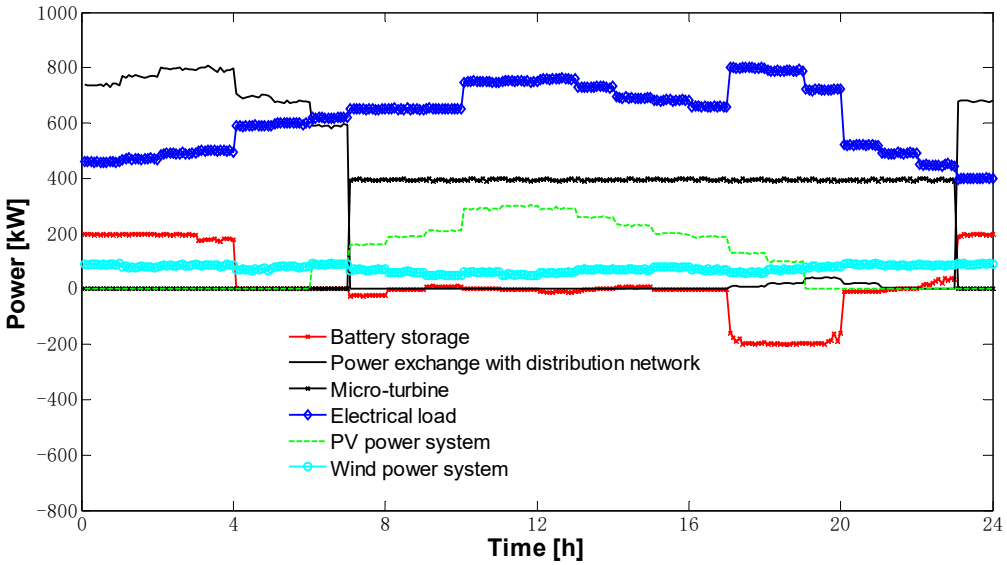

(**b**)

Figure 10. The electrical load balance curves of a typical day in winter (**a**) and summer (**b**) under real-time optimal dispatching mode.

The heating load balance curves of a typical day in winter (Figure 11a) and the cooling load balance curves of a typical day in summer (Figure 11b) under real-time optimal dispatching mode are

shown in Figure 11. Similar to Figure 10, the state of the energy-supply units related to the heating load (Figure 11a) in winter and cooling load (Figure 11b) in summer follows the operating strategy of the day-ahead optimal dispatch. Compared with the day-ahead optimal dispatch in Figure 9, the output power of each energy-supply unit is accurate, and the power variation of each energy-supply unit is smaller. Thus, safe operation of the system is guaranteed. The system can respond quickly to changes in cooling and heating loads, thereby further improving the applicability of the system.

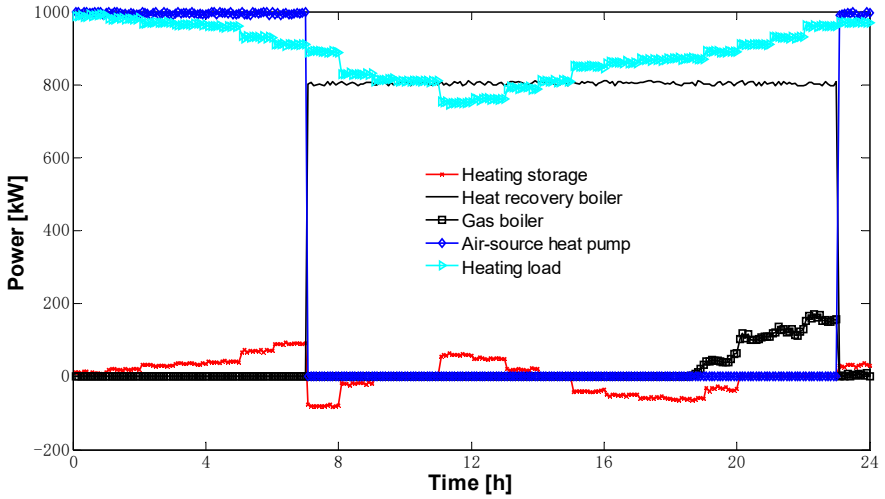

(**a**)

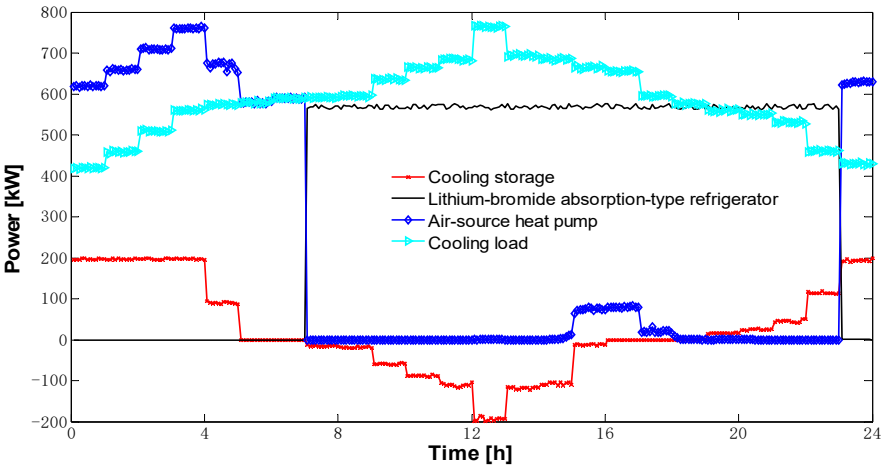

(**b**)

Figure 11. The heating load balance curves of a typical day in winter (**a**) and the cooling load balance curves of a typical day in summer (**b**) under real-time optimal dispatching mode.

5.3. Comparison of Optimal Results between the Day-Ahead Optimal Dispatch and the Real-Time Optimal Dispatch

The comparison of electricity-supply units (Figure 12a) and heating-supply units (Figure 12b) in winter between the day-ahead optimal dispatch and real-time optimal dispatch are shown in Figure 12. The comparison of electricity-supply units (Figure 13a) and cooling-supply units (Figure 13b) in summer between the day-ahead optimal dispatch and real-time optimal dispatch are shown in Figure 13. Compared with the day-ahead predictive data for the wind and PV power generation system, and the cooling-heating-electricity load in Figure 6, the intraday ultra-short-term predictive data for the wind and PV power generation system, and the cooling-heating-electricity load in Figure 7 has small fluctuations. The day-ahead predictive data are used in the day-ahead optimal dispatch,

and the intraday ultra-short-term predictive data are used in the real-time optimal dispatch. According to the comparison of optimal results between the day-ahead optimal dispatch and the real-time optimal dispatch in Figures 12 and 13, the energy-supply units in the real-time optimal dispatch can respond to the power variations of the wind and PV power generation system, and the cooling-heating-electricity load in real time. The validity of proposed method in this paper is further verified.

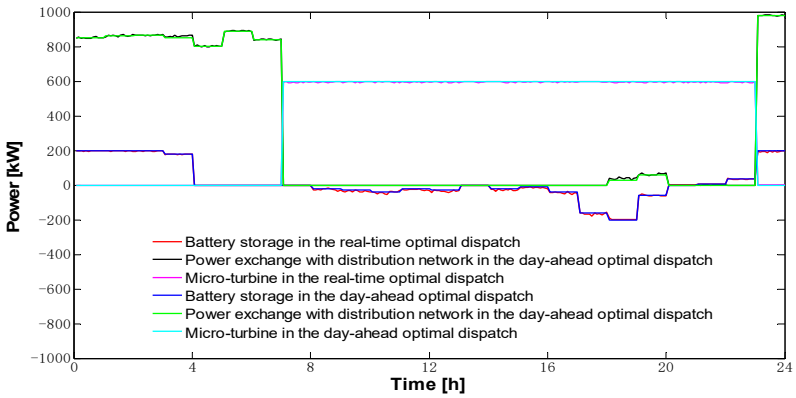

(**a**)

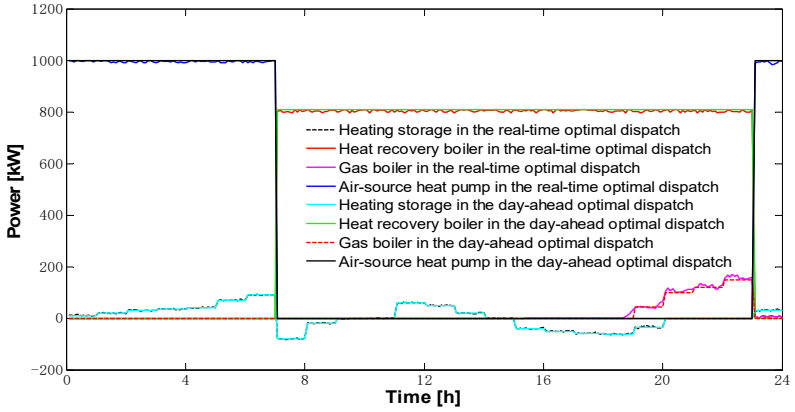

(**b**)

Figure 12. Comparison of electricity-supply units (**a**) and heating-supply units (**b**) in winter between the day-ahead optimal dispatch and the real-time optimal dispatch.

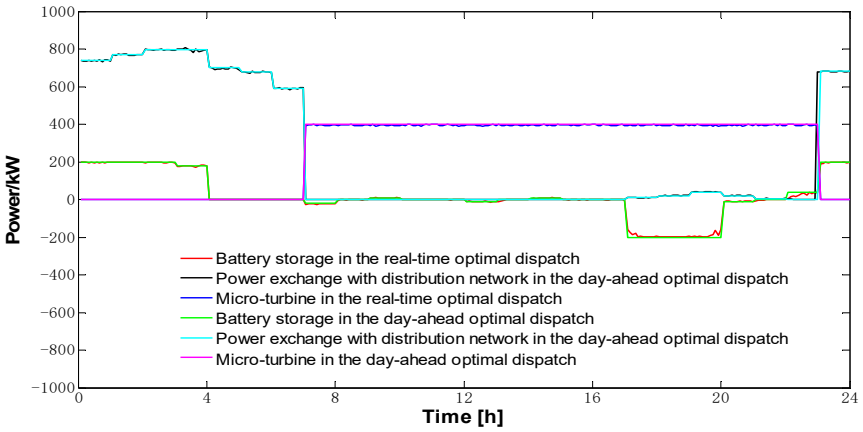

(**a**)

Figure 13. *Cont.*

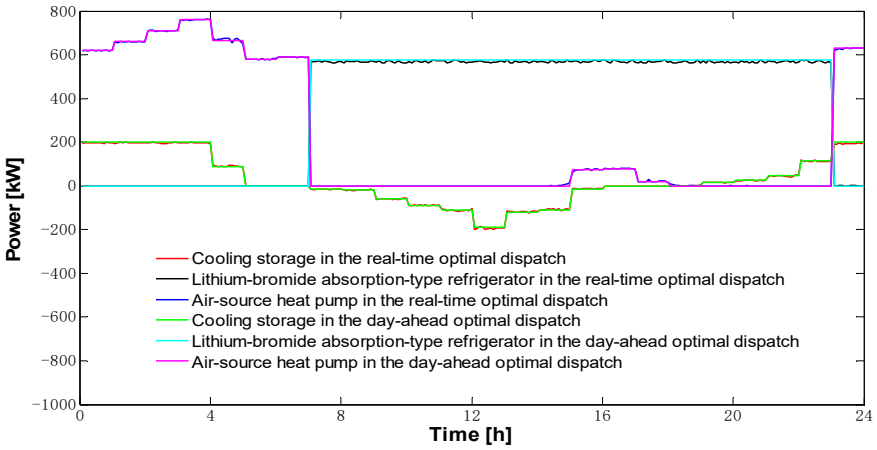

(**b**)

Figure 13. Comparison of electricity-supply units (**a**) and cooling-supply units (**b**) in summer between the day-ahead optimal dispatch and real-time optimal dispatch.

6. Conclusions

An integrated optimal dispatching method based on model predictive control for a rural micro-energy-grid is proposed in this paper to address the randomness of the intermittent distributed energy output and load demand. The integrated optimal dispatching method includes the day-ahead optimal dispatch and real-time optimal dispatch. In the day-ahead optimal dispatch, the optimal dispatch model of the micro-energy-grid is built taking the daily minimum operating cost as the objective function, and the output power curve of each micro-source is obtained on an hourly time scale. In the real-time optimal dispatch, the rolling optimization of the day-ahead optimal dispatching plan is implemented based on model predictive control theory. The real-time state of the system is sampled, and feedback correction of the system is implemented to achieve smooth operation of the system. According to the simulated case study, the state of the energy-supply units in the micro-energy-grid maintains the operating strategy of the day-ahead optimal dispatch. The output power of each energy-supply unit is accurate, and output power variables of the units are small. The safe operation of the system is guaranteed, and the system can respond rapidly to fluctuations in the output power of renewable energy and the electricity-cooling-heating load. The applicability of the system is further extended.

In the next step, intraday ultra-short-term renewable energy generation and prediction of electricity-cooling-heating load are strengthened, and the optimal dispatching model of the micro-energy-grid is more detailed. The operating dispatching plan more closely fits the actual operating conditions of the system to promote the rapid development of micro-energy-grid technology.

Author Contributions: J.Y. and M.Z. proposed the topic of the study and designed the research framework. T.J. and X.Z. established mathematical model of study and performed case simulation. W.W. analyzed the data. X.Z. wrote the final paper.

Funding: This research was funded by the Headquarters Science and Technology Projects from the State Grid Corporation of China (Grant No. 5227221600KQ).

Conflicts of Interest: The authors declare no conflict of interest.

Nomenclature

Variables

$C_{electri}$	difference between the cost of purchasing electricity and the income of selling electricity for the micro-energy-grid
$C_{maintain}$	maintenance cost of the micro-energy-grid
$C_{pollution}$	cost of environmental pollution

C_{gas}	cost of purchasing biogas
$e_1(t)$	electricity purchasing price of the micro-energy-grid
$e_2(t)$	electricity selling price of the micro-energy-grid
$P_{\text{ex}}(t)$	power exchange between the micro-energy-grid and the distribution network (purchasing electricity power is positive, and selling electricity power is negative)
$P_{\text{EB}}(t)$	heating power of the heat-recovery boiler
$P_{\text{GB}}(t)$	heating power of the biogas-fired boiler
$P_{\text{estor}}(t)$	electrical power of the battery storage device (discharge is negative and charge is positive)
$P_{\text{MT}}(t)$	electrical power of the micro-turbine
$P_{\text{PV}}(t)$	electrical power of the PV power generation system
$P_{\text{WT}}(t)$	electrical power of the wind power generation system
$P_{\text{AC}}(t)$	cooling power of the lithium-bromide absorption-type refrigerator
$P_{\text{hstor}}(t)$	heating power of the heating storage device (discharge is negative, and charge is positive)
$P_{\text{cstor}}(t)$	cooling power of the cooling storage device (discharge is negative, and charge is positive)
$P_{\text{electriload}}(t)$	electrical load
$P_{\text{ASHP}}(t)$	electrical power of the air-source heat pump
$P_{\text{CASHP}}(t)$	cooling power of the air-source heat pump
$P_{\text{HASHP}}(t)$	heating power of the air-source heat pump
$P_{\text{heatingload}}(t)$	heating load
$P_{\text{coolingload}}(t)$	cooling load
C_{fuel}	biogas price
C_y	penalty of pollutant gas y
D_y	environmental value of pollutant gas y
B_y	emission value of pollutant gas y
m	type of pollutant gas
C_{mEB}	maintenance cost of the heat-recovery boiler
C_{mGB}	maintenance cost of the biogas-fired boiler
C_{mestor1}	cost for storing energy in the battery storage device
C_{mestor2}	daily manual maintenance cost of the battery storage device
C_{mMT}	maintenance cost of the micro-turbine
C_{mPV}	maintenance cost of the PV power generation system
C_{mWT}	maintenance cost of the wind power generation system
C_{mAC}	maintenance cost of the lithium-bromide absorption-type refrigerators
C_{mASHP}	maintenance cost of the air-source heat pump
C_{mhstor}	maintenance cost of the heating storage device
C_{mcstor}	maintenance cost of the cooling storage device
$P_{\text{MT}}^{\text{max}}$	maximum electrical power of the micro-turbine
$P_{\text{EB}}^{\text{max}}$	maximum heating power of the heat-recovery boiler
$P_{\text{GB}}^{\text{max}}$	maximum heating power of the biogas-fired boiler
$P_{\text{AC}}^{\text{max}}$	maximum cooling power of the lithium-bromide absorption-type refrigerator
$R_{\text{MT}}^{\text{down}}$	downward climbing speed of the micro-turbine
$R_{\text{MT}}^{\text{up}}$	upward climbing speed of the micro-turbine
$R_{\text{GB}}^{\text{down}}$	downward climbing speed of the biogas-fired boiler
$R_{\text{GB}}^{\text{up}}$	upward climbing speed of the biogas-fired boiler
η_{e}	value of the power generation efficiency of the micro-turbine
η_1	value of the heating loss coefficient of the micro-turbine
η_{rec}	value of the recovery efficiency of the flue gas waste heat
η_{EB}	efficiency of the heat-recovery boiler
η_{AC}	efficiency of the lithium-bromide absorption-type refrigerator
$S_{\text{stor}}(\text{t})$	state of charge of the cooling–heating–electricity storage device
δ	self-discharging efficiency of the cooling–heating–electricity storage device
$P_{\text{ch}}(t)$	charging power of the cooling–heating–electricity storage device

$P_{\mathrm{dis}}(t)$	discharging power of the cooling–heating–electricity storage device
η_{ch}	charging efficiencies of the cooling–heating–electricity storage device
η_{dis}	discharging efficiencies of the cooling–heating–electricity storage device
ΔT	dispatching period
E_{tstor}	total capacity of the cooling–heating–electricity storage device
$S_{\mathrm{stor}}^{\min}$	minimum state of charge of the cooling–heating–electricity storage device
$S_{\mathrm{stor}}^{\max}$	maximum state of charge of the cooling–heating–electricity storage device
P_{cmax}	maximum charging power of the cooling–heating–electricity storage device
P_{dmax}	maximum discharging power of the cooling–heating–electricity storage device
P_{stor}	charging and discharging power of the cooling–heating–electricity storage device
D_{CASHP}	cooling efficiency of the air-source heat pump
D_{HASHP}	heating efficiency of the air-source heat pump
$P_{\mathrm{ASHP}}^{\max}$	maximum electrical power of the air-source heat pump
$P_{\mathrm{ex}}^{\min}$	minimum power exchange between the micro-energy-grid and the distribution network
$P_{\mathrm{ex}}^{\max}$	maximum power exchange between the micro-energy-grid and the distribution network
Y_{res}	system reserve rate
$\Delta P_{\mathrm{EB}}(k+t)$	power variation in the heat-recovery boiler
$\Delta P_{\mathrm{GB}}(k+t)$	power variation in the biogas-fired boiler
$\Delta P_{\mathrm{AC}}(k+t)$	power variation in the lithium-bromide absorption-type refrigerator
$\Delta P_{\mathrm{MT}}(k+t)$	power variation in the micro-turbine
$\Delta P_{\mathrm{ASHP}}(k+t)$	power variation in the air-source heat pump
$\Delta P_{\mathrm{WT}}(k+t)$	power variation in the wind power generation system
$\Delta P_{\mathrm{PV}}(k+t)$	power variation in the PV generation system
$\Delta P_{\mathrm{electriload}}(k+t)$	power variation in the electrical load
C_{estor}	cost for storing energy in the battery storage device
$e_3(t)$	electricity selling price of the PV and wind power generation system
$e_4(t)$	electricity selling price of the micro-turbine
$\hat{P}_{\mathrm{ex}}(k+t)$	power exchange between the micro-energy-grid and the distribution network in the day-ahead optimal dispatch
$\hat{P}_{\mathrm{estor}}(k+t)$	charging and discharging power of the battery storage device in the day-ahead optimal dispatch
$\hat{S}_{\mathrm{estor}}(k+t)$	state of charge of the battery storage device in the day-ahead optimal dispatch
$\hat{P}_{\mathrm{cstor}}(k+t)$	charging and discharging power of the cooling storage device in the day-ahead optimal dispatch
$\hat{S}_{\mathrm{cstor}}(k+t)$	state of charge of the cooling storage device in the day-ahead optimal dispatch
$\hat{P}_{\mathrm{hstor}}(k+t)$	charging and discharging power of the heating storage device in the day-ahead optimal dispatch
$\hat{S}_{\mathrm{hstor}}(k+t)$	state of charge of the heating storage device in the day-ahead optimal dispatch
$\hat{P}_{\mathrm{EB}}(k+t)$	power of the heat-recovery boiler in the day-ahead optimal dispatch
$\hat{P}_{\mathrm{GB}}(k+t)$	power of the biogas-fired boiler in the day-ahead optimal dispatch
$\hat{P}_{\mathrm{AC}}(k+t)$	power of the lithium-bromide absorption-type refrigerator in the day-ahead optimal dispatch
$\hat{P}_{\mathrm{MT}}(k+t)$	power of the micro-turbine in the day-ahead optimal dispatch
$\hat{P}_{\mathrm{ASHP}}(k+t)$	power of the air-source heat pump in the day-ahead optimal dispatch
$\Delta P_{\mathrm{EB}}^{\min}$	minimum power variation in the heat-recovery boiler
$\Delta P_{\mathrm{EB}}^{\max}$	maximum power variation in the heat-recovery boiler
$\Delta P_{\mathrm{GB}}^{\min}$	minimum power variation in the biogas-fired boiler
$\Delta P_{\mathrm{GB}}^{\max}$	maximum power variation in the biogas-fired boiler
$\Delta P_{\mathrm{AC}}^{\min}$	minimum power variation in the lithium-bromide absorption-type refrigerator
$\Delta P_{\mathrm{AC}}^{\max}$	maximum power variation in the lithium-bromide absorption-type refrigerator

$\Delta P_{\mathrm{MT}}^{\min}$	minimum power variation in the micro-turbine
$\Delta P_{\mathrm{MT}}^{\max}$	maximum power variation in the micro-turbine
$\Delta P_{\mathrm{ASHP}}^{\min}$	minimum power variation in the air-source heat pump
$\Delta P_{\mathrm{ASHP}}^{\max}$	maximum power variation in the air-source heat pump
$\Delta P_{\mathrm{estor}}^{\min}$	minimum charging and discharging power variation in the battery storage device
$\Delta P_{\mathrm{estor}}^{\max}$	maximum charging and discharging power variation in the battery storage device
$\Delta P_{\mathrm{cstor}}^{\min}$	minimum charging and discharging power variation in the cooling storage device
$\Delta P_{\mathrm{cstor}}^{\max}$	maximum charging and discharging power variation in the cooling storage device
$\Delta P_{\mathrm{hstor}}^{\min}$	minimum charging and discharging power variation in the heating storage device
$\Delta P_{\mathrm{hstor}}^{\max}$	maximum charging and discharging power variation in the heating storage device
$P_{\mathrm{estor}}^{\max}$	maximum charging and discharging power of the battery storage device
$P_{\mathrm{estor}}^{\min}$	minimum charging and discharging power of the battery storage device
$P_{\mathrm{cstor}}^{\max}$	maximum charging and discharging power of the cooling storage device
$P_{\mathrm{cstor}}^{\min}$	minimum charging and discharging power of the cooling storage device
$P_{\mathrm{hstor}}^{\max}$	maximum charging and discharging power of the heating storage device
$P_{\mathrm{hstor}}^{\min}$	minimum charging and discharging power of the heating storage device
$S_{\mathrm{estor}}^{\min}$	minimum state of charge of the battery storage device
$S_{\mathrm{estor}}^{\max}$	maximum state of charge of the battery storage device
$S_{\mathrm{cstor}}^{\min}$	minimum state of charge of the cooling storage device
$S_{\mathrm{cstor}}^{\max}$	maximum state of charge of the cooling storage device
$S_{\mathrm{hstor}}^{\min}$	minimum state of charge of the heating storage device
$S_{\mathrm{hstor}}^{\max}$	maximum state of charge of the heating storage device
E_{testor}	total capacity of electricity storage device
E_{tcstor}	total capacity of cooling storage device
E_{thstor}	total capacity of heating storage device
σ_{estor}	self-discharging efficiency of the battery storage device
σ_{cstor}	self-discharging efficiency of the cooling storage device
σ_{hstor}	self-discharging efficiency of the heating storage device
η_{estor}	charging and discharging efficiency of the battery storage device
η_{cstor}	charging and discharging efficiency of the cooling storage device
η_{hstor}	charging and discharging efficiency of the heating storage device

Abbreviations

PV	photovoltaic

References

1. He, Y.B.; Yan, M.Y.; Shahidehpour, M.; Li, Z.Y.; Guo, C.X.; Wu, L.; Ding, Y. Decentralized optimization of multi-area electricity-natural gas flows based on cone reformulation. *IEEE Trans. Power Syst.* **2018**, *33*, 4531–4542. [CrossRef]
2. Rashidi, H.; Khorshidi, J. Exergoeconomic analysis and optimization of a solar based multigeneration system using multiobjective differential evolution algorithm. *J. Clean. Prod.* **2018**, *170*, 978–990. [CrossRef]
3. Li, Y.; Yang, Z.; Li, G.Q.; Zhao, D.B.; Tian, W. Optimal scheduling of an isolated microgrid with battery storage considering load and renewable generation uncertainties. *IEEE Trans. Ind. Electron.* **2019**, *66*, 1565–1575. [CrossRef]
4. Hosseinzadeh, M.; Salmasi, F.R. Fault-tolerant supervisory controller for a hybrid ac/dc micro-grid. *IEEE Trans. Smart Grid* **2018**, *9*, 2809–2823. [CrossRef]
5. Jeremy, R. *Third Industrial Revolution: How Lateral Power Is Transforming Energy, the Economy, and the World*; Palgrave Macmillan Trade: New York, NY, USA, 2011; pp. 33–72.
6. Fu, X.Q.; Zhang, X.R. Failure probability estimation of gas supply using the central moment method in an integrated energy system. *Appl. Energy* **2018**, *219*, 1–10. [CrossRef]
7. Li, Z.M.; Xu, Y. Optimal coordinated energy dispatch of a multi-energy microgrid in grid-connected and islanded modes. *Appl. Energy* **2018**, *210*, 974–986. [CrossRef]

8. Mi, Y.; Liu, H.Y.; Song, G.X.; Li, Z.Q.; Fu, Y.; Li, Z.K. Two-layer power optimization allocation of multi-energy local networks oriented to energy internet. *Power Autom. Equip.* **2018**, *38*, 1–10.
9. Ding, T.; Mu, C.L.; Bie, Z.H.; Du, P.W.; Fan, Z.Y.; Zou, Z.X.; Yang, Y.H.; Wu, Z.Y.; Xu, Y.; Tang, B.G. Review of energy internet and its operation. *Proc. CSEE* **2018**, *38*, 4318–4328.
10. Chen, S.; Wei, Z.N.; Sun, G.G.; Sun, Y.L.; Zang, H.X.; Zhu, Y. Optimal power and gas how with a limited number of control actions. *IEEE Trans. Smart Grid* **2018**, *9*, 5371–5380. [CrossRef]
11. Habibollahzade, A.; Gholamian, E.; Ahmadi, P.; Behzadi, A. Multi-criteria optimization of an integrated energy system with thermoelectric generator, parabolic trough solar collector and electrolysis for hydrogen production. *Int. J. Hydrog. Energy* **2018**, *43*, 14140–14157. [CrossRef]
12. Qiu, J.; Zhao, J.H.; Yang, H.M.; Wang, D.X.; Dong, Z.Y. Planning of solar photovoltaics, battery energy storage system and gas micro turbine for coupled micro energy grids. *Appl. Energy* **2018**, *219*, 361–369. [CrossRef]
13. Meesenburg, W.; Ommen, T.; Elmegaard, B. Dynamic exergoconomic analysis of a heat pump system used for ancillary services in an integrated energy system. *Energy* **2018**, *152*, 154–165. [CrossRef]
14. Li, S.X.; Hu, M.H.; Gong, C.C.; Zhan, S.; Qin, D.T. Energy Management Strategy for Hybrid Electric Vehicle Based on Driving Condition Identification Using KGA-Means. *Energies* **2018**, *11*, 1531. [CrossRef]
15. Hosseinzadeh, M.; Salmasi, F.R. Robust Optimal Power Management System for a Hybrid AC/DC Micro-Grid. *IEEE Trans. Sustain. Energy* **2015**, *6*, 675–687. [CrossRef]
16. Zhang, X.; Yang, J.H.; Wang, W.Z.; Jing, T.J.; Zhang, M. Optimal operation analysis of the distribution network comprising a micro energy grid based on an improved grey wolf optimization algorithm. *Appl. Sci.* **2018**, *8*, 923. [CrossRef]
17. Chan, D.; Cameron, M.; Yoon, Y. Implementation of micro energy grid: A case study of a sustainable community in China. *Energy Build.* **2017**, *139*, 719–731. [CrossRef]
18. Wang, H.; Ai, Q.; Wu, J.H.; Xie, Y.Z.; Zhou, X.Q. Bi-level distributed optimization for microgrid clusters based on alternating direction method of multipliers. *Power Syst. Technol.* **2018**, *42*, 1718–1727.
19. Yang, L.J.; Li, H.Q.; Yu, X.Y.; Zhao, J.S.; Liu, W.Y. Multi-objective day-ahead optimal scheduling of isolated microgrid considering flexibility. *Power Syst. Technol.* **2018**, *42*, 1432–1440.
20. Bharothu, J.N.; Sridhar, M.; Rao, R.S. Modified adaptive differential evolution based optimal operation and security of AC-DC microgrid systems. *Int. J. Electr. Power Energy Syst.* **2018**, *103*, 185–202. [CrossRef]
21. Gao, R.; Wu, J.; Hu, W.; Zhang, Y. An improved ABC algorithm for energy management of microgrid. *Int. J. Comput. Commun. Control* **2018**, *13*, 477–491. [CrossRef]
22. Hemmati, M.; Mohammadi-Ivatloo, B.; Ghasemzadeh, S.; Reihani, E. Risk- based optimal scheduling of reconfigurable smart renewable energy based microgrids. *Int. J. Electr. Power Energy Syst.* **2018**, *101*, 415–428. [CrossRef]
23. Chen, G.; Yang, Q. An ADMM-based distributed algorithm for economic dispatch in islanded microgrids. *IEEE Trans. Ind. Inform.* **2018**, *14*, 3892–3903. [CrossRef]
24. Lu, X.H.; Zhou, K.L.; Yang, S.L.; Liu, H.Z. Multi-objective optimal load dispatch of microgrid with stochastic access of electric vehicles. *J. Clean. Prod.* **2018**, *195*, 187–199. [CrossRef]
25. Ma, T.F.; Wu, J.Y.; Hao, L.L. Energy flow modeling and optimal operation analysis of the micro energy grid based on energy hub. *Energy Convers. Manag.* **2017**, *133*, 292–306. [CrossRef]
26. Lin, K.J.; Wu, J.Y.; Hao, L.L.; Liu, D.; Li, D.Z.; Yan, H.G. Optimization of operation strategy for micro-energy grid with cchp systems based on non-cooperative game. *Autom. Electr. Power Syst.* **2018**, *42*, 25–32.
27. Ghasmi, A.; Banejad, M.; Rahimiyan, M. Integrated energy scheduling under uncertainty in a micro energy grid. *IET Gener. Transm. Distrib.* **2018**, *12*, 2887–2896. [CrossRef]
28. Li, D.Z.; Wu, J.Y.; Shi, K.; Ma, T.F.; Zhang, Y.; Zhang, R.Y. Bi-level optimal dispatch model for micro energy grid based laod aggregator business. In Proceedings of the 2017 IEEE Conference on Energy Internet and Energy System Integration (EI2), Beijing, China, 26–28 November 2017; pp. 643–648.
29. Wang, W.Z.; Liu, F.C.; Zheng, J.J.; Yanf, Y.; Zhang, J.H.; Yang, J.H.; Jing, T.J. Optimal regulation on micro energy grid based on time-shifting agricultural load. In Proceedings of the 2017 IEEE Conference on Energy Internet and Energy System Integration (EI2), Beijing, China, 26–28 November 2017; pp. 42–47.
30. Wang, Y.Z.; Niu, H.N.; Yang, L.; Wang, W.Z.; Liu, F.C. An optimization method for local consumption of photovoltaic powr in a facility agriculture micro energy network. *Energies* **2018**, *11*, 1503. [CrossRef]
31. Wu, X.; Wang, X.L.; Bie, Z.H.; Wang, J.X. Economic operation of microgrid with combined heat and power system. *Electr. Power Autom. Equip.* **2013**, *33*, 1–6.

32. Xu, Q.S.; Zeng, A.D.; Wang, K.; Jiang, L. Day-ahead optimized economic dispatching for combined cooling, heating and power in micro energy-grid based on hessian interior point method. *Power Syst. Technol.* **2016**, *40*, 1657–1665.
33. Zhao, J.; Yang, H.H.; Ye, D.F.; Qing, W.C. Research on energy system based on CCHP coupled with energy storage. *Energy Convers. Technol.* **2016**, *34*, 120–124.
34. Wang, C.; Gu, W.; Wu, Z. Economic and optimal operation of a combined heat and power micro grid with renewable energy resources. *Autom. Electr. Power Syst.* **2011**, *35*, 22–27.
35. Ma, X.Y.; Wu, Y.W.; Fang, H.L.; Sun, Y.Z. Optimal sizing of hybrid solar-wind distributed generation in an islanded microgrid using improved bacterial foraging algorithm. *Proc. CSEE* **2011**, *31*, 17–25.
36. Xian, X.; Fan, C.G.; Wen, S.S.; Wang, Y.C.; Chen, C.; Liu, X. Optimal deployment for island microgrid considering probabilistic factors of renewable energy generations. *Eng. J. Wuhan Univ.* **2016**, *49*, 101–104.
37. Pazouki, S.; Haghifam, M.R.; Moser, A. Uncertainty modeling in optimal operation of energy hub in presence of wind, storage and demand response. *Int. J. Electr. Power Energy Syst.* **2014**, *61*, 335–345. [CrossRef]